First-principles calculation of *p*-type doping of ZnSe using nitrogen

S. Gundel and W. Faschinger
Lehrstuhl für Experimentelle Physik III der Universität Würzburg, Am Hubland, D-97074 Würzburg, Germany
(Received 15 November 2000; revised manuscript received 28 March 2001; published 26 December 2001)

We have employed first-principles density-functional calculations to describe the behavior of nitrogen as a *p*-type dopant in ZnSe. Our previous finding that the nitrogen acceptor decays by migrating from a substitutional site to a neighboring interstitial site, is described in further detail. In particular the mechanism that accounts for the superior stability of the decayed acceptor is described. We also examine the diffusion of the point defects that result from the decay of the acceptor, which have been found to be responsible for the degradation of ZnSe-based devices. Furthermore we pay attention to the behavior of a N_2 molecule within the ZnSe matrix, and to alternative doping strategies that utilize codoping with Cl or In. While the introduction of Cl does not remove the instability of the nitrogen acceptor, codoping with In may provide a means to prevent the degradation of the dopant. We conclude by presenting similar simulations for ZnTe that show the absence of the aforementioned decay mechanism, and refer to experimental results from a ZnTe based diode.

DOI: 10.1103/PhysRevB.65.035208 PACS number(s): 61.72.Vv, 61.72.Ji, 61.72.Yx, 71.55.Gs

I. INTRODUCTION

During the last few years nitrogen has been unrivaled as the standard *p*-type dopant for II-VI semiconductors such as ZnSe. However, the commercial distribution of ZnSe-based devices has been hampered by their limited lifetime that could not be prolonged past a few hundred hours for blue-green laser diodes.[1] While stacking faults were initially considered as the main cause of device degradation, it was recently found that even fault-free devices suffer from a homogeneous darkening that finally leads to the destruction of the device.[2,3]

Considerable theoretical effort has been spent in the past years on the proposition of compensating defect structures that decrease the concentration of free charge carriers in nitrogen-doped ZnSe. Among the first to considered the decay of the nitrogen acceptor were Van de Walle *et al.*,[4] who stated that N on Zn or interstitial sites should be quite improbable, and favored a complex of interstitial Zn and substitutional N_{Se}. Detailed calculations of the formation energy of this defect complex were made by Pöykkö *et al.*,[5] who confirmed its low formation energy, compared, e.g., with that of the N_{Se}^{-} defect. However, theoretical works showed that the equilibrium density of Zn interstitials is very low,[6] Furthermore molecular-beam-epitaxy growth of nitrogen-doped ZnSe is usually performed under Se rich conditions, rendering the formation of Zn interstitials improbable. Thus the Zn_i-N_{Se} complex is, despite its stability, an unlikely candidate for compensation.

Particular attention has been paid to the possibility of self compensation in ZnSe by the formation of positively charged Se vacancies. Among the first to consider these explicitly were Laks *et al.*,[6] who calculated formation energies for all native point defects in ZnSe in a variety of charge states. They found that self-compensation should play no major role in stoichiometric ZnSe. In nonstoichiometric ZnSe self-compensation should be *n* type as well as *p*-type, failing to explain the difficulty of *p* type ZnSe doping at all. García and Northrup[7] stated that the Se vacancy could in principle play a role in compensation, but would most probably be superseded by the formation of defect complexes involving interstitial Zn.

Cheong *et al.*[8] proposed the appearance of a N_2 molecule at a Se site, or the formation of a split-interstitial N-N complex as another possible compensating defect. They also commented on a self-compensation mechanism initially proposed by Chadi and Chang[9] for As or P as a *p*-type dopant. They suggested the relaxation of the dopant atom from the substitutional toward the interstitial site which would result in a positively charged point defect. Cheong *et al.* stated that such a defect could only become metastable in a positively charged state.

Although theory has favored substitutional nitrogen together with other interstitial atoms as the dominating compensating defect for *p*-type doping in ZnSe, there have been hints from experiments that let interstitial nitrogen appear as a possibility to be considered. Kubo[10] studied the preferred nitrogen location on a ZnSe surface grown by molecular-beam epitaxy using He^{1+} and Ne^{1+} scattering. He recognized the substitutional Se site as the preferred adsorption site, while excess nitrogen would locate at interstitial sites. The dopant site in bulk ZnSe was investigated by Kobayashi *et al.*[11] using ion-beam analysis. They found a large fraction of the detected nitrogen is randomly distributed. Upon a decrease of the dopant activation ratio the fractions of nitrogen at random sites as well as at interstitial sites increases. Tournié *et al.*[12] found signatures of a shallow donor in nitrogen-doped ZnSe that they attributed to interstitial nitrogen.

The authors of this paper recently proposed a compensation that involves the migration of a nitrogen dopant atom from substitutional Se to a neighboring interstitial site.[13] The resulting defect complex acts as a donor that is most stable in the higher positive $+3$ charge state and, as is shown in this paper, in the $+5$ charge state. This complex is conceptually very simple, since it neither requires the pre-existence of native point defects nor involves the migration of other atoms towards dopant sites, and is capable of explaining the observed gradual decay of initially functional devices.[14] This mechanism is described in greater detail here, and an expla-

nation is offered for why this compensating defect is energetically favorable in very high charge states. We have also investigated the behavior of N_2 molecules in ZnSe, and studied possible strategies for codoping as a means to suppress the deactivation of the *p*-type dopant. Among these only codoping with In may provide a remedy for the intrinsic instability of the nitrogen acceptor. On the other hand, this instability does not seem to prevail in ZnTe. Attempts to fabricate light-emitting diodes containing Te suggest an alternative to ZnSe devices, since they do not show significant degradation despite high defect densities.[15]

II. DETAILS OF THE CALCULATION

For our calculations of defect formation energies in ZnSe we employed density-functional theory (DFT)[16] within the local-density approximation (LDA), together with self-consistent pseudopotentials in a plane-wave basis. For the LDA the parametrization of Perdew and Zunger, based on calculations by Ceperley and Alder, was employed.[17] The accurate simulation of the nitrogen atoms necessitated the expansion of the single-particle wave functions in plane waves with a cutoff energy of 30 Ry.

All configurations were simulated within a cubic supercell, being eqivalent to a $2\times2\times2$ cubic unit cell and containing 64 atoms, with periodic boundary conditions being applied. For integrations in **k** space a mesh of $2\times2\times2$ special **k** points in the full reciprocal cell was employed, being equivalent to 64 **k** points in the cubic unit cell or 256 **k** points in the primitive unit cell. The atoms at the sidefaces of the cubic supercell were fixed at their ideal bulk positions while all others were allowed to relax under self-consistently calculated forces.[18] All the simulations presented in this paper were done with the ''fhi96md'' simulation package.[19]

The pseudopotentials for the involved species were generated in a mixed scheme that utilized the prescriptions by Hamann[20] and Troullier and Martins.[21] For the Zn pseudopotential the nonlinear core correction of Louie *et al.*[22] was employed. We found that for Zn, Se, and Te, smooth pseudopotentials could be obtained by choosing potentials of the Troullier-Martins type for the *s* and *p* components and of the Hamann type for the local *d* component. All pseudopotentials were carefully checked in order to exclude ''ghost states.[23]'' The pseudopotential generation and checking were done using the package ''fhi98pp'' that is distributed by the Fritz Haber Institute.[24]

The pseudopotentials for Zn and Se were optimized with respect to the elastic properties of ZnSe bulk. We found an equilibrium lattice constant of 5.588 Å and elastic constants $C_{11}=0.928$ Mbar and $C_{12}=0.530$ Mbar. Allowing for the typical LDA overbinding, these are in reasonable agreement with the respective experimental values of 5.668 Å, 0.895 Mbar, and 0.539 Mbar.[25] However, the self-consistently calculated heat of formation of 0.61 eV severely underestimates the experimental value of about 1.65 eV.[7] While testing different pseudopotentials, we found that this discrepancy can be mainly attributed to the Se pseudopotential. On the other hand, a Se pseudopotential that allows for a more accurate heat of formation overestimates the elastic constant C_{11} while underestimating C_{12}. Expecting a considerable relaxation of the ZnSe lattice in the vicinity of the nitrogen atom, we chose the combination of pseudopotentials which provides the most accurate elastic constants.

For ZnTe we found an equilibrium lattice constant of 5.97 Å and elastic constants $C_{11}=0.722$ Mbar and $C_{12}=0.422$ Mbar, to be compared with 6.10 Å, 0.713 Mbar, and 0.407 Mbar.[25] Simulating the vibration of a diatomic nitrogen molecule, we obtained an equilibrium separation of 1.121 Å and a vibration frequency of 70.24 THz with our pseudopotential. The respective experimental values are 1.098 Å and 70.70 THz.[26]

Since charged systems were simulated in this work, a charge compensation scheme was necessary in order to prevent Coulomb repulsion due to the periodic boundary conditions. This was ensured by setting the monopole moment of the electrostatic interaction (or, equivalently, the charge density at $\mathbf{G}=\mathbf{0}$ in reciprocal space) to zero. While this choice makes the supercell appear as an electrically neutral cube, electrostatic interactions remain to be considered.[27,28] The corrections applied to the defect energies in this work are explained in detail in the Appendix.

The formation energies Ω_D of the nitrogen related defects were evaluated using the standard expression

$$\Omega_D = E_D + Q_D\mu_e - n_N\mu_N, \tag{1}$$

where E_D and Q_D are the total energy and charge of a supercell, respectively, and μ_e is the chemical potential of the electrons relative to the valence band edge. n_N and μ_N denote the chemical potential and of nitrogen and the number of nitrogen atoms in one supercell. The energies E_D were corrected for band alignment and differences in the effective potential of the supercell outside the defect region. However, due to the extended nature of the doping complex in the supercell and more complex energy band structures, an uncertainty of about 0.1 eV arose from this procedure, which is of the order of the corrections applied. Since the numbers of Zn and Se atoms in the supercell do not change, it is feasible not to consider them explicitly.

This scheme also allows for estimating the transition levels between different charge states of one kind of impurity complex. The scheme underlying this kind of evaluation is described in great detail in Ref. 6. It is based on the supposition that at a given value of the electronic chemical potential μ_e the charge state associated with the lowest energy will actually form. When two lines, denoting different charge states of the same defect, intersect, the most stable charge state of the defect changes. It is expected that this charge state will be assumed subsequently, involving the exchange of charge with the host crystal.

As an alternative to this scheme the observation of changes in the density of filled states with different charge states could be used to identify the defect states. However, this approach suffers from the underestimation of band gaps and bandwidths typical of classical DFT. The band gap of ZnSe was found to be 1.26 eV in our calculations, about half of the value known from experiments. The approach to defect level energies used in this work does not rely on the

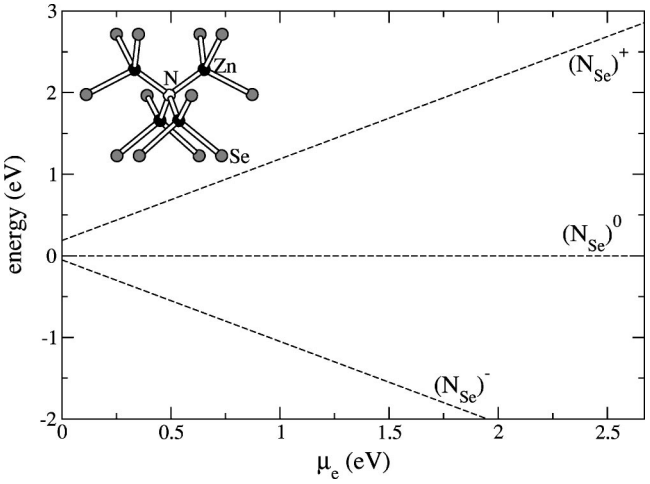

FIG. 1. Formation energies for a nitrogen atom at a substitutional Se site for different charge states. The energy of the neutral atom was chosen as the reference energy.

notion of band gaps, but uses differences of ground-state energies for different numbers of electrons instead. Effects related to the aforementioned band-gap underestimation manifest themselves here through their impact on the total energy. The correctness of the defect level energies thereby depends on the accuracy of the predicted formation energies of the related defects. Errors in the formation energies would be reflected on the defect levels. On the other hand, comparing the defect levels thus obtained with excitation energies known from experiments offers a simple measure for the reliability of the theoretical results.

Figure 3 shows how the energies of three transitions between the $5+$, $3+$, $2+$, and $1+$ states of the (N_i-V_{Se}) complexes are determined. These energies are given by the abscissae of the crossing points of the respective lines that are marked by the vertical dashed lines. Another example can be found in Ref. 6. We do not suggest denoting crossings between lines referring to different defect complexes as transition levels, since such a crossing would also require a change in the atomic structure of the defect.

When selecting charge states for the doping complexes we frequently omitted those leaving an unpaired electron in the supercell, especially when simulating complexes that comprise vacancylike voids. An unpaired electron in conjunction with such a vacancy would lead to a half-filled orbital, and thus to a degenerate ground state. This is mainly due to problems arising from the simulation of defect complexes whose precise atomic structure is unknown. When a simulation proceeded from an essentially guessed atomic configuration toward the simultaneous electronic and structural ground state, sometimes convergence was lost when the ordering of the electronic levels was changed. The presence of an unpaired electron aggravated this situation considerably.

It is known that some electronic systems undergo distortions in order to remove such a degenerate ground state. Examples of these Jahn-Teller distortions are frequently found with molecules or reconstructed surfaces. Although this appears to be true also for some instances of defects in solids, e.g., the Se vacancy,[7] charge states with unpaired electrons are not always energetically unfavorable, as will be shown below in Fig. 3. On the other hand the basic statement about the instability of the nitrogen acceptor is not impaired by this omission. Therefore, in most cases presented below only charge states with an even number of valence electrons in the supercell will be considered.

III. DECAY OF THE NITROGEN ACCEPTOR

In this section we compare the formation energies of the nitrogen acceptor at the substitutional Se site with those of a decayed complex, consisting of a Se vacancy and the nitrogen atom that previously occupied this site but migrated to a neighboring interstitial site. We also estimate the migration barrier for the transition of the nitrogen atom for different charge states.

A. Nitrogen at the substitutional site

A nitrogen atom at a substitutional Se site should be most stable when carrying one negative charge, thus acting as an ionized acceptor. We have calculated the formation energies of this point defect for different charge states, according to Eq. (1). The formation energy of the neutral substitutional N atom was chosen to serve as the reference energy. The resulting energies are shown in Fig. 1. Here, for a given electronic chemical potential, the lowest line identifies the most stable configuration. The abscissa gives the location of the electronic chemical potential, occasionally referred to as the Fermi level, zero denoting the valence-band maximum. As described in Sec. II, the abscissae where two lines representing different charge states of one defect intersect denote defect levels within the band gap. Since the acceptor level of nitrogen in ZnSe is known to be located about 0.11 eV above the valence-band edge,[29] the lines denoted N_{Se}^{0} and N_{Se}^{1-} should intersect there. However, in Fig. 1 they intersect about 0.05 eV below the valence-band edge. Since this discrepancy cannot be resolved within the basic assumptions that this work is built upon, we have to take it as a measure of the error margin for our calculations.

The atoms around the substitutional nitrogen site show a considerable inward (breathing) relaxation due to the small covalent radius of the nitrogen atom. The lengths of the N-Zn bond are 1.993, 1.990, and 1.998 Å for the -1, neutral, and $+1$ charge states. The bonds from the Zn atoms in the first shell around the N atom to the Se atoms in the second shell are 2.51 Å long, independent of the investigated charge states. Similar bond lengths were already reported by Kwak *et al.*[30] For reference, the Zn-Se bond length at our self-consistently calculated lattice constant is 2.42 Å. In analogy to Ref. 30, we have calculated the spatial distribution of the uppermost occupied electron states for the singly negatively charged substitutional nitrogen atom. In contrast Ref. 30, we find that the charge density of the two uppermost occupied states is quite localized around the substitutional nitrogen atom instead of the neighboring Se atoms, as shown in Fig. 2.

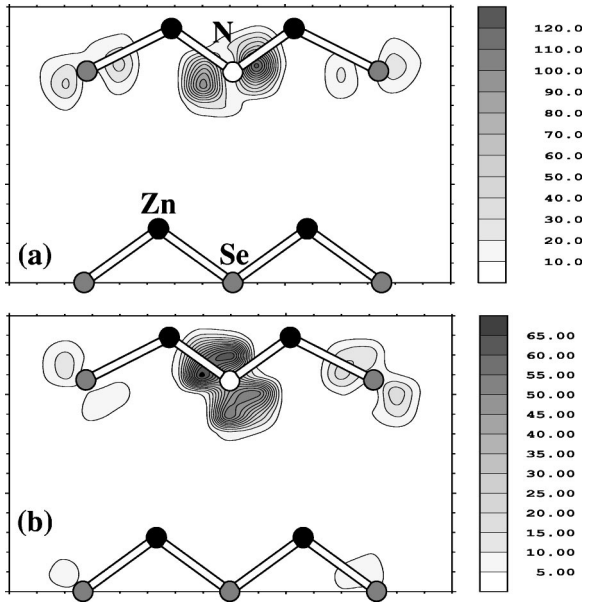

FIG. 2. Charge density of the second highest (a) and highest occupied state for a nitrogen atom at the substitutional site.

B. Nitrogen at the interstitial site

In an earlier publication[13] we pointed out that a complex consisting of a Se vacancy and a nitrogen atom in a neighboring interstitial site is more stable in a triply positive charge state than the negatively charged substitutional acceptor, thus acting as a compensator for *p*-type doping. At this point we generalize this statement to multiply positively charged complexes. Figure 3 shows the formation energies as functions of the electronic chemical potential for charge states up to $+7$. One can see that in the regime below $\mu_e = 0.26$ eV the defect complex formed by a Se vacancy and an interstitial nitrogen atom is the most stable one. For reference the formation energies from Fig. 1 are shown as dashed lines. To our knowledge, such high charge states have not yet been proposed for point defects. However, as we shall explain in Sec. III B 1, charge states up to $+5$ are stabilized by charge depletion at Zn atoms surrounding the nitrogen site, thus leading to a more extended defect complex.

Since, according to Fig. 3, the positively charged (N_i-V_{Se}) complexes are more stable than the substitutional nitrogen acceptor as soon as the Fermi energy approaches the valence band edge, in thermodynamic equilibrium the formation of the acceptor is highly improbable. The fact that, nevertheless, high acceptor concentrations are achieved experimentally indicates that some kinetic limitaton dominates the complex formation. This can be understood if one considers that the original concentration of Se vacancies is very low.[6] Thus nitrogen must first be incorporated substitutionally. This is in accordance with the experimental observation of Kubo *et al.*[10] that the substitutional Se site is the preferred adsorption site for nitrogen on a ZnSe growth surface. The formation of the (N_i-V_{Se}) complex can thus be understood as a decay of pre-existing nitrogen acceptors. Since the moving nitrogen atom creates the necessary Se vacancy, no pre-existing vacancies are needed in this process.

The decay process is, however, decelerated by two effects: as we will show below, the nitrogen atom has to overcome an energy barrier to reach the stable interstitial position. Even more important, the originally negatively charged acceptor has to change its charge state to form positive (N_i-V_{Se}) complexes, which requires a considerable input of energy. Thus the decay of the *p*-type dopant does not take place spontaneously but on a considerable time scale and under external influences like illumination with high-energy photons or current injection.

1. Electronic structure

The migration of the nitrogen atom from the substitutional to the interstitial site proceeds along the [111] direction. Adhering to the observation of a negligible Jahn-Teller distortion for substitutional nitrogen,[30] we assume that the threefold rotational symmetry around this axis is preserved during the migration process. The relaxation of the host lattice around the defect site is nevertheless much more complicated than in the substitutional case. During the migration the N-Zn bond along the migration direction is broken, and a large lattice relaxation follows similar to that proposed by Chadi and Chang.[9] However, the nitrogen atom does not stop in the plane spanned by the three other neighboring Zn atoms, but moves beyond until the remaining N-Zn bonds are also broken and three N-Se bonds are formed. Geometry data for the defect featuring interstitial nitrogen are presented for different charge states in Table I.

The Zn atoms formerly bound to the nitrogen move outward, changing their hybridization from sp^3 to sp^2. This can clearly be seen from the sum of the bond angles around these atoms that are shown in the middle column (left) of Table I. These angles sum up to almost 360° for $+5$, $+3$, and $+2$

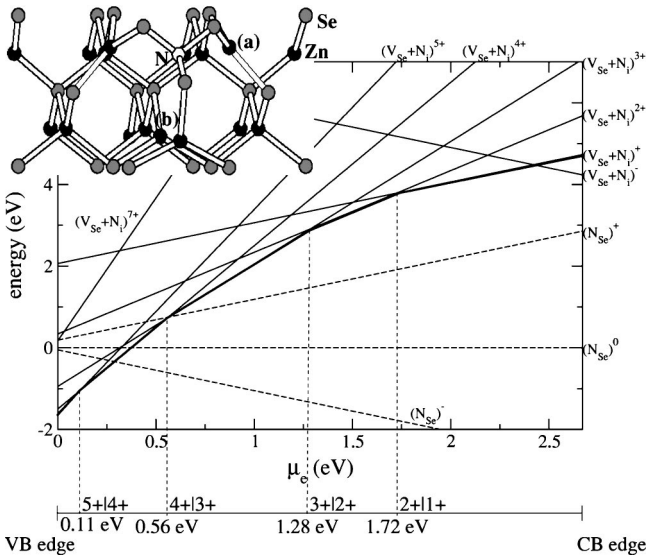

FIG. 3. Formation energies for a nitrogen atom at an interstitial site near a Se vacancy for different charge states. The energies from Fig. 1 are shown in dashed lines. The bar below the panel represents the ZnSe band gap. Dashed lines denote the locations of the defect levels in the gap and their connection with the crossings between formation energy lines.

TABLE I. Geometric data for the point defect formed by the nitrogen atom at the interstitial site. Angles are in degrees, bond lengths in Å. The two angle sums for the Zn atom refer to a Zn atom connected to the interstitial N via one Se atom (middle column, left; a in Fig. 3) and to the Zn atom opposite to the N atom (middle column, right; b in Fig. 3). The right column gives the N-Se bond length and the angle between two such bonds (here all bond angles are equal).

Charge state	Sum of Zn bond angles	N-Se bond length / bond angle
−1	355.36 / 344.97	1.908 / 108.13
+1	342.18 / 298.74	1.873 / 112.45
+2	357.34 / 350.19	1.883 / 109.80
+3	357.96 / 354.96	1.874 / 110.85
+5	359.35 / 355.44	1.783 / 109.38

charge states. For an sp^3-hybridized atom this value would be about 328.5°. In Fig. 4 the density distributions of the highest occupied single particle states for the +5 and +3 cases are depicted. It is interesting to note that, irrespective of the highly positive charge of the complex as a whole, in both cases a considerable amount of negative charge is localized at the nitrogen atom. This suggests that the charge depletion that must occur for the highly positively charged defects does not take place at the nitrogen atom itself, but rather elsewhere.

At the charge state +1 the Zn atoms surrounding the vacancy move inward, indicating that the additional negative charge is located near the Se vacancy. This can be seen in Fig. 5, which shows that at this charge state the highest occupied orbital is concentrated at the nitrogen atom, while part of its charge has moved to the opposing Zn atom.

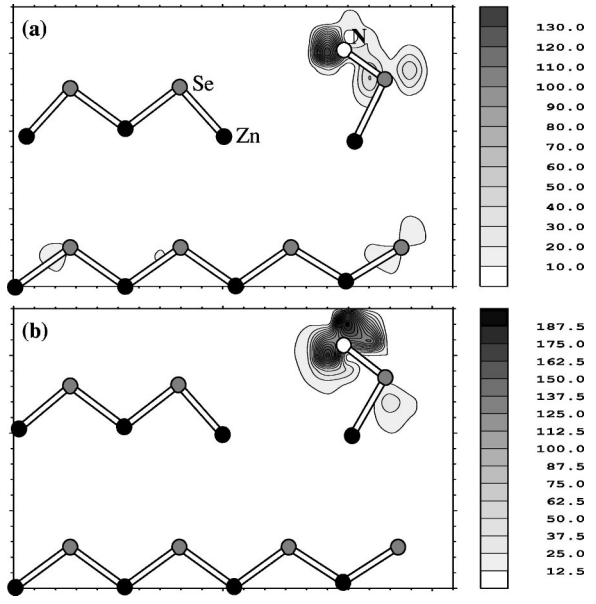

FIG. 4. Density distributions of single-electron states: (a) density of the hightest occupied state for the charge state +5; (b) same for the charge state +3. The density contours are in electrons per supercell.

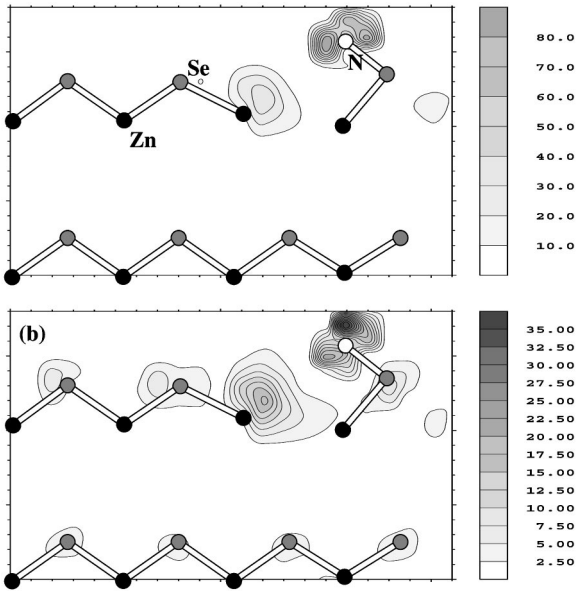

FIG. 5. Density distributions of single-electron states for the charge state +1: (a) density of the hightest occupied state; (b) density of the lowest unoccupied state. The density contours are in electrons per supercell.

At the charge state −1 the Zn atoms move outward again, hinting that the newly introduced negative charge has also been distributed over the Zn atoms, causing Coulomb repulsion. This behavior can be inferred from the plot of the distribution of the lowest unoccupied state for the charge state +1 in Fig. 5.

For comparison we have also added the formation energy of the charge state +7. In Fig. 3 this charge state is higher in energy than the substitutional −1 state over the whole range of the electronic chemical potential μ_e so that its formation is very unlikely. We also abstain from discussing this charge state in further detail, as we will show below that the $(N_i\text{-}V_{\mathrm{Se}})$ complex becomes more and more extended spatially with increasing positive charge. Therefore, an even larger supercell would be required to obtain a proper description of the defect, which is outside our computational means. Finally the objective of this paper, i.e., to report on the instability of the nitrogen acceptor in ZnSe, is not affected by this omission.

Figure 6 shows the integral densities of filled states for interstitial nitrogen at the charge states +1, +3, and +5. The inset features an enlarged view of the region around the valence-band edge. From this inset the location of the less positively charged states along the energy axis can be inferred. Obviously the emergence of interstitial nitrogen is connected to the formation of deep levels in the band gap. The underestimation of the band gap within the LDA formalism hinders a direct evaluation of the defect level energies from this picture. Regarding the full panel, it is interesting to note that minor features of the fivefold positively charged system are shifted toward lower energies while the major features are still congruent with their counterparts at the lower charge states. This includes the peaks at −7.5, −11.5, −15, and −20.5 eV. Thus the increased stability of

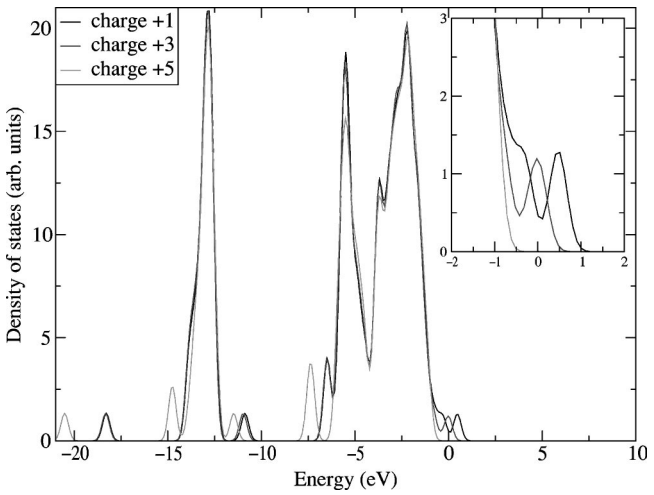

FIG. 6. Densities of filled states for interstitial N at the charge state $+1$, $+3$, and $+5$ in comparison. The inset shows the valence-band-edge region. The energy scale is centered at the valence-band edge in the center of the Brillouin zone.

the charge state $+5$ results not only from the charge depletion at the valence-band edge but also from the shift of states well below the valence-band edge toward lower energies.

The change in the integral density of states can be qualitatively understood from Fig. 7. In the upper panel the Zn atom pointed to by the outer arrow is mainly sp^3 hybridized, since it resides close to the position that it would occupy in an undistorted lattice. In the lower panel the three bonds projecting from the same atom are almost coplanar, indicating that in this case the Zn atom is mainly sp^2 hybridized. The observation that the N-Se bond is considerably shorter in the $+5$ case than in the $+3$ case (cf. Table I) also fits in this picture. In the $+3$ case the sp^3-like hybridization of the aforementioned Zn atoms suggests the existence of Zn-Se backbonds to the Se atoms connected to the nitrogen atom. These backbonds stretch the N-Se bonds, leading to a fivefold coordination of the Se atoms. The further removal of charge in the transition to the $+5$ case breaks these backbonds, leading to shorter N-Se bonds.

To summarize, in the case of the charge states $+3$ and $+5$ the charges of the highest occupied orbitals are concentrated around the interstitial nitrogen atom. During the transition from $+3$ to $+5$, the Zn atoms to which the Se atoms closest to the N atom were backbonded change their hybridization from sp^3 to sp^2. The charge that was located in the bonds is delivered to the host lattice. Thus the charge concentration around the nitrogen atom does not change significantly. When moving from $+3$ to $+1$ and -1, the newly introduced charge is located near the Zn atoms surrounding the Se vacancy.

2. Formation of the defect

Formation energy profiles for different charge states as functions of the nitrogen location during the migration process are depicted in Fig. 8. In this figure the left edge of the abscissa denotes the substitutional position, while a value of 0.5 denotes the interstitial position that is finally occupied by

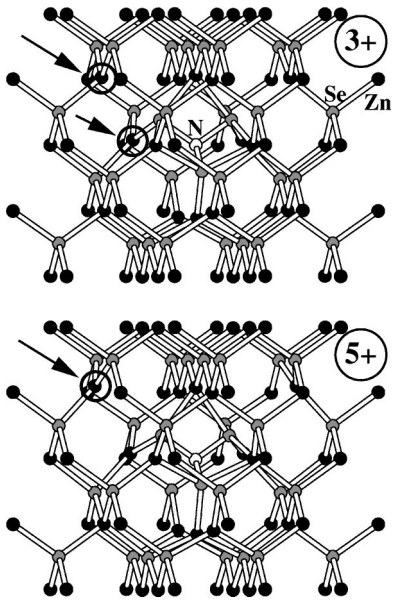

FIG. 7. Ball-and-stick models for the interstitial nitrogen-related defect giving an extended view of the lattice structure. In the upper panel (charge state $+3$) the Zn atom indicated by the upper arrow is evidently sp^3 hybridized, while in the lower panel the same atom is sp^2 hybridized.

the nitrogen atom. When the nitrogen atom moves away from the substitutional site one of the N-Zn bonds breaks. This accounts for the initial energy barrier for the migration. When the nitrogen atom has crossed the plane spanned by

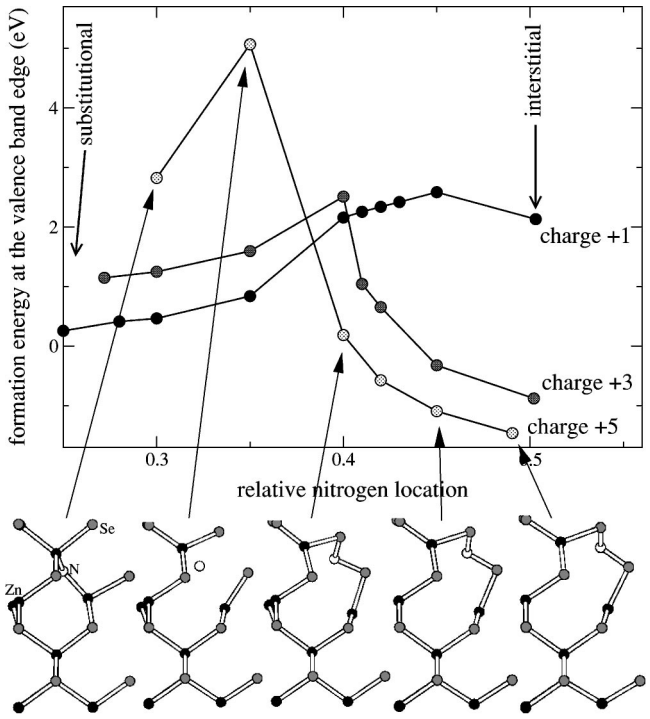

FIG. 8. Formation energy profiles during the migration of a nitrogen atom from a substitutional site to a interstitial site for the charge states $+1$, $+3$, and $+5$. All energies are plotted for $\mu_e = 0$, i.e., with the Fermi level located at the valence-band edge.

the other three Zn atoms, N-Se bonds are formed which induce a decrease in the defect energy for the charge states $+3$ and $+5$. In the case of the charge state $+1$ the defect energy remains almost constant.

The driving force for the migration of substitutional nitrogen to an interstitial site is obviously the strength of the N-Se bond. In the $+5$ charge state seven Zn atoms have changed their hybridization from sp^3 to mainly sp^2, while three N-Se bonds were formed. It is known that the strength of this bond in a diatomic molecule is 3.84 eV.[26] For the compound Se_4N_4 a bond energy of 2.56 ± 0.43 eV has been published.[31] Unfortunately, to our knowledge no similar data for the N-Zn bond are available for comparison. Thus we can only estimate the energy per bond for a Zn_3N_2 crystal. This crystal is known to appear in the bixbyite structure.[32] In this structure each metal atom is surrounded by four nonmetal atoms. From this we conclude that for each Zn atom four Zn-N bonds exist. By dividing the formation energy of Zn_3N_2 from its gaseous compounds by the expected number of Zn-N bonds, we arrive at a value of 1.175 eV per bond. This is significantly lower than the strength of the N-Se bond even in the Se_4N_4 compound, and explains quite easily the superior stability of interstitial nitrogen even if the host lattice is strongly distorted as a consequence.

All three lines in the upper panel of Fig. 8 are drawn under the assumption that $\mu_e = 0$, which means that the Fermi level is located at the valence-band edge. In the case of a higher electronic chemical potential, the three curves are shifted upward by different degrees, depending on the charge state: as can be inferred from Eq. (1), the upward shift will be proportional to the charge of the defect. This implies that, the greater the number that nitrogen atoms have already moved to interstitial sites, barrier for nitrogen migration will be. This can be seen as a self-limiting effect on the generation of donorlike defect comlexes. For instance, the energy of the fivefold positive defect is about 0.66 eV lower than that of the threefold positive complex at $\mu_e = 0$, but both are equal in energy when the Fermi level is located 0.33 eV above the valence-band edge.

Obviously the height of the barrier for the migration of a nitrogen atom depends on the charge of the resulting complex. For a threefold positive complex the barrier height is about 2.51 eV. This barrier agrees well with the energy of photons emitted by a ZnSe-based laser (about 2.5 eV). Optical degradation experiments on stacking fault-free regions of lasers show that degradation starts only if photons with energies higher than 2.4 eV are used, and that a photon energy of about 2.6 eV is needed to obtain strong degradation.[2] However, the energy profiles in Fig. 8 implicitly assume that the defects are positively charged from the beginning, and do not change their charges during the migration of the nitrogen atom. In addition to the barriers in Fig. 8, the change of the charge state from -1 (nitrogen acceptor) to $+3$ is a second limiting mechanism for the formation of the N_i-V_{Se} complex.

As explained above, the crossing points of the lines for the different positively charged complexes in Fig. 3 can be used to deduce that the energy levels of these defect complexes lie near the middle of the band gap. The limiting step in the charge-transfer process is thus the removal of the first electron from the acceptor to the conduction band, for which an energy corresponding to E_{Gap}-E_A, or 2.6 eV, is needed. In a properly designed device where *p*-type doping is done in a ZnMgSSe cladding layer with an energy gap of about 2.9 eV while the laser emission from the CdZnSe well is around 2.5 eV, the value of E_{Gap}-E_A can be considerably larger than the energy of the photons emitted by the device. However, a formation of deep defects, together with a drastic decrease in the free hole concentration, has been observed even for properly designed, stacking fault free devices with CW lifetimes higher than 100 h.[3] Thus a decay of the acceptor takes place even in high quality samples. The most probable mechanism is an energy transfer to the acceptor from overshooting electrons which recombine in the cladding layer either radiatively or by multiphonon emission.

In the case of the fivefold positively charged complex the migration barrier in Fig. 8 is more than 3 eV and consequently higher than the energy of overshooting electrons. If such highly charged complexes indeed form during the degradation of a diode, this could only occur via the intermediate formation of a threefold positive complex, from which additional charge is removed in a second step.

As a final detail concerning the formation of the decayed nitrogen acceptor we mention that the correction scheme for the energies of the charged defects requires to assume a certain concentration of free charge carriers (see the Appendix). The reason for this is that we assume the screening of the ionized dopant sites to depend on the Debye length which in turn depends on the charge carrier concentration. Since the screening length will be the shorter, the higher concentration of free charge carriers will be, the stability of the decayed nitrogen acceptor will probably depend on this as well, and the rate of decay will in turn depend on the dopant concentration initially present in the crystal.

In Fig. 9 the energies of three most prominent instances of the defects from Fig. 3 are shown for four different assumed charge-carrier concentrations (the correction scheme of Leslie and Gillan corresponds in fact to no free charge carriers at all; also see, the Appendix). As can be seen, the intact and decayed nitrogen complexes are approximately equal in energy at $\mu_e \rightarrow 0$ when the hole concentration is around 1×10^{16} cm^{-3}. This agrees with data from aging experiments on ZnSe-based laser diodes. In Ref. 3 it was found that the effective carrier concentration in a laser diode was diminished from about 7×10^{16} cm^{-3} initially to about 5×10^{15} cm^{-3} after aging. It appears that in the device under investigation the aging process came to a halt after the hole concentration dropped under a certain limiting value. This value allowing for the range of uncertainty imminient in the model of degradation studied here, is in reasonable agreement with the limiting charge carrier concentration derived from Fig. 9. We take this congruence as a hint that (1) the degradation mechanism for the nitrogen acceptor presented in this paper is confirmed by experiments, and (2) the charge-carrier-dependent correction of the defect energies taken from simulations is reasonable.

IV. DIFFUSION OF THE RESULTING POINT DEFECTS

In Ref. 13 we discussed the role of the degradation of nitrogen doping in ZnSe in the observed degradation of

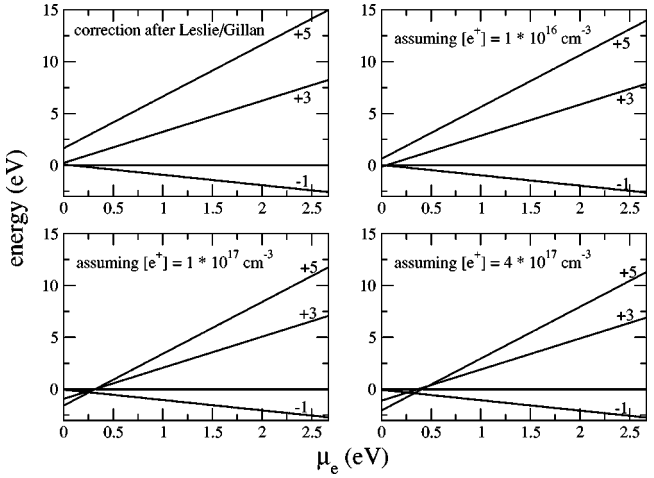

FIG. 9. Defect energies of prominent instances of the defects depicted in Fig. 3. The line labeled "−1" denotes an ionized nitrogen acceptor, while lines "+3" and "+5" correspond to a decayed acceptor at the two indicated charge states. The corrections applied to the defect energies taken from simulations are listed in Table III.

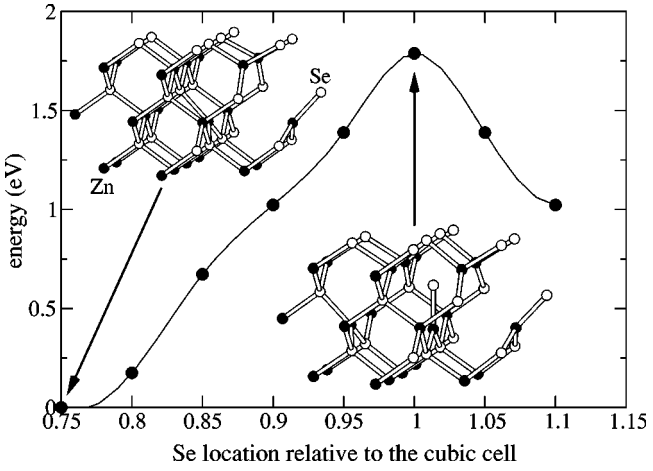

FIG. 10. Energy profile for the diffusion of an isolated Se vacancy as a function of the Se position. The dots denote calculated energies, while the solid line is obtained by a cubic spline interpolation. The abscissa 0.75 denotes the traveling Se atom at its ideal bulk position, while 1.0 denotes the intermediate position between two bulk sites.

ZnSe-based laser diodes. We pointed out that while the degradation of a ZnSe based laser diode is initiated by the nitrogen dopant in the *p* layer, the final destruction of the quantum well is caused by the diffusion of positively charged point defects toward it.

Degradation measurements were performed at small stacking-fault-free mesas which were irradiated with laser light at a photon energy of 2.71 eV, corresponding to the energy gap of the waveguide layer of the laser diode. The quantum-well intensity was furthermore measured as a function of time under an electric field that was applied in reverse bias direction. When this field was applied, the degradation rate of the laser diode decreased by a factor of about 3. The experiments showed that radiation enhanced defect reactions can be ruled out as the mechanism for the reduced degradation, leaving the diffusion of a positively charged species against the applied field as the most probable explanation.

In order to establish a relation between the applied field and the change in the degradation rate a formula introduced by Kimerling[33] was applied. The change in the diffusion barrier was evaluated as $\Delta E = q \times F \times x$ for a defect with charge q in an electric field F over a distance x between a minimum and a maximum in the diffusion potential. Based on this expression a change in the diffusion rate by a factor of $\exp(-\Delta E/k_B T) \simeq 0.36$ was found at room temperature, close to the value derived from the experiment. Nevertheless the nature of the positively charged diffusing species cannot be deduced from the experiment. It would be tempting to assume that this species is in fact the (N_i-V_{Se}) complex.

In order to investigate if this is plausible, in the present work a twofold way is chosen. First the diffusion barrier for an isolated Se vacancy is determined from *ab initio* simulations. All simulation parameters were chosen as described above, except the plane-wave cutoff energy which was reduced to 10 Ry. This is possible since the computationally expensive modelling of a nitrogen atom is not necessary here. For the diffusion process the defect was assumed to remain twofold positively charged. The defect energy as a function of the position of the diffusing Se atom is shown in Fig. 10. This figure features the energy associated with a diffusing Se atom as a function of the precise location of the diffusing atom during the migration of a Se atom from its natural site in the ZnSe lattice toward a neighboring Se vacancy. Since this migration implies the relocation of the vacancy, this is at the same time the migration potential for a Se vacancy in ZnSe. It is implicitly assumed that during this transition the charge +2 of the Se vacancy, which is known to be the most stable charge state of this defect in *p*-type doped ZnSe,[7] is retained. From these data the diffusion barrier is evaluated to 1.79 eV. This value is smaller by a factor of 2 compared to the result of a study undertaken by Chen *et al.*,[34] who reported a migration energy of 4.0 eV for the same defect, though conceding that the migration energies of anion vacancies in compound semiconductors are generally about 2 eV.

From Fig. 10 it can be deduced that the separation between the minimum and maximum of the diffusion potential is 0.203 nm. If we take this distance together with the charge +2 of the Se vacancy and an electric field of 6×10^7 V/m from Ref. 13 and assume room temperature, we also arrive at a reduction of the diffusion rate by a factor of about 0.36. We note here that this situation is given only near the edge of the intrinsic region (which enlarges toward the *p*-type doped region when a reverse voltage is applied). Since this is only a crude estimate, the congruence may be seen as fortuitous. Nevertheless we regard it as an additional hint that the diffusing species is actually the twofold positively charged Se vacancy.

Second the total energies of a nitrogen atom in two different interstitial sites without neighboring vacancies were obtained from simulations. At this point the interstitial positions of the nitrogen atom inside a Zn tetrahedron and a Se tetrahedron were considered with charge states +1 and +3. In order to facilitate a comparison with the (N_i-V_{Se}) complex

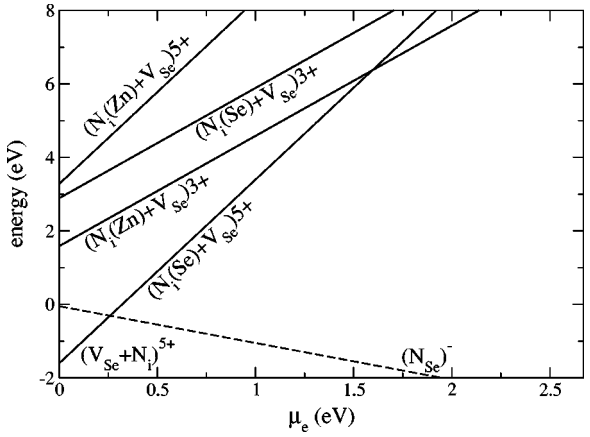

FIG. 11. Formation energies for two independent defects: a twofold positively charged Se vacancy combined with a N interstitial with charge +1 or +3. The dashed lines denote complexes that already appeared in Fig. 3 and were added for comparison.

discussed above, we combined these total energies with that of a twofold positive, isolated Se vacancy and subtracted the energy of an appropriate amount of ZnSe bulk in order to adjust the numbers of atoms. The resulting charges are therefore +3 and +5, as indicated. The obtained formation energies are shown in Fig. 11 as a function of the electronic chemical potential μ_e. As can be seen, the sum of energies of the Se vacancy and the isolated nitrogen interstitial in a Se neighborhood is equal to the $(N_i+V_{\mathrm{Se}})^{5+}$ complex; the two lines denoting these cases cannot be distinguished from each other in Fig. 11. This suggests that the interstitial nitrogen and the accompanying Se vacancy can separate from each other without the need to overcome a substantial barrier.

Figure 11 also shows that the formation energy of the interstitial nitrogen within a Zn tetrahedron is almost 4.9 eV higher than that within a Se tetrahedron, if both carry a fivefold positive charge. The $(N_i+V_{\mathrm{Zn}})^{3+}$ complex lies about 3.2 eV above the $(N_i+V_{\mathrm{Se}})^{5+}$ complex. In the case of the Zn tetrahedron the host lattice is only slightly disturbed by the interstital atom. Additional stabilization through the formation of bonds does not take place. If the nitrogen atom were assumed to diffuse through the ZnSe lattice via interstitial positions it would always have to visit a Zn tetrahedron site between two Se tetrahedron sites. Thus the migration barrier would be at least the aforementioned 3.2 eV if charge is exchanged with the host lattice, and 4.9 eV if not. Since even the lower of these values surpasses the barrier for Se vacancy migration by about 1.3 eV we again conclude that the migrating defect that leads to the observed final destruction of ZnSe based laser diodes is in fact a Se vacancy and not the $(N_i$-$V_{\mathrm{Se}})$ complex as a whole.

V. MOLECULAR NITROGEN

A common side effect of the use of a plasma cell for nitrogen doping is the introduction of N_2 molecules into the growing crystal. Since such a point defect cannot be supposed to be electrically inactive, we found it instructive to include it in the set of simulations presented in this work.

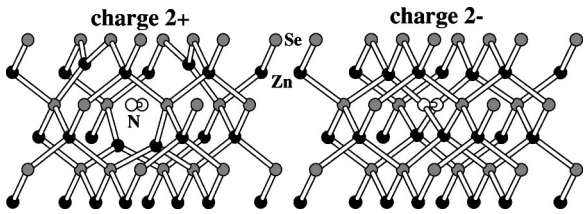

FIG. 12. Ball-and-stick models for a N_2 dimer at a Se site for the charge states +2 and −2.

Charge states of +2, 0, and −2 have been considered. Regarding the host crystal as a reservoir for unpaired electrons, we again regard the occurrence of half-filled orbitals as highly improbable.

It turns out that the appearance of a N_2 molecule at a substitutional Se site results in two different behaviors, depending on the charge state. These modes can be observed in Fig. 12, while the most important geometric data are compilated in Table II. When the defect is twofold positively charged, the Zn atoms surrounding the site move outward until they reside almost within the plane spanned by the respective three Se atoms they are bound to. This signifies a change in the hybridization of these Zn atoms from sp^3 to sp^2, and indicates that the positive charge of the defect is distributed evenly over them while the N_2 dimer remains inactive.

In the case of neutral and twofold negative defects the distortion of the lattice around the N_2 molecule is much smaller. In these cases the bond configuration of the surrounding Zn atoms indicates that the nitrogen atoms are actually bound to the Zn atoms, thus destabilizing the N_2 molecule by minimizing the overlap of the π orbitals centered at the N atoms that contain the additional electrons. Consequently the substitutional N_2 dimer is much less stable in these charge states.

The formation energies of the N_2 molecule at the Se site for the three charge states under consideration are presented in Fig. 13. Because of the difficulty of fixing an appropriate value for the chemical potential of nitrogen μ_{N}, each line representing a charge state for N_2 appears twice: first μ_{N} was derived from the total energy of an isolated N_2 molecule that was simulated self-consistently, such as has already been done by Pöykkö *et al.*[5] In the second place μ_{N}, as proposed by Cheong *et al.*,[8] was used: they assumed a dense N_2 gas with half of the molecules in the first excited state, adding 1.545 eV to the chemical potential of a nitrogen atom.

TABLE II. Geometric data for a substitutional N_2 molecule for different charge states. The middle column gives the separation between the two nitrogen atoms, while the right column contains the distance between the actual position of a Zn atom next to the dimer and its ideal bulk position.

Charge state	N-N separation (Å)	Zn relaxation (Å)
+2	1.130	0.630
0	1.235	0.105
−2	1.235	0.130

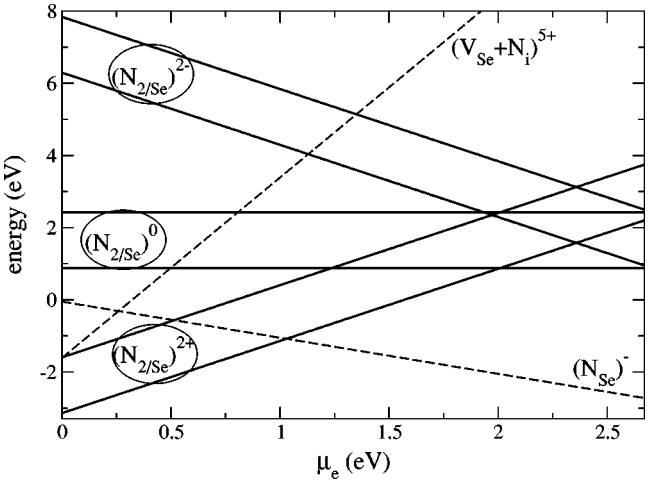

FIG. 13. Formation energies for a substitutional N_2 molecule at the charge states $+2$, 0, and -2. Dashed lines refer to the respective energies for single nitrogen atoms that already appeared in Fig. 3. Solid lines denote the N_2 molecules. Due to differing prescriptions for the calculation of the chemical potential for nitrogen in the literature, each solid line appears twice: the upper line of each set refers to the chemical potential for nitrogen as given by the energy of an isolated N_2 molecule, the lower assumes the value of μ_N proposed in Ref. 8 (see the text).

Figure 13 shows that a nitrogen dimer at a Se site in the ZnSe lattice is surprisingly stable when carrying two positive charges, even if the maximum value of μ_N is considered. At charge states of 0 and -2 this defect plays only a minor role. Due to its charge state it also acts as a donor, and is thus capable of compensating for the atomic nitrogen acceptor. Since nitrogen atoms in the ZnSe host lattice do not show a noticeable tendency to migrate, as described above, we think that this defect is not very important at moderate nitrogen concentrations. However, it will become important at high nitrogen concentrations or if only excited N_2 molecules are used for doping, as, e.g., with a low power dc plasma. In fact, very low free hole concentrations have been obtained for both cases[35]

Cheong *et al.*[8] proposed a split interstitial N-N complex, carrying two positive charges, to be considerably prominent, where one nitrogen atom occupies a Se site while the other is located in an interstitial position along the [100] direction. However, since Fig. 12 shows that the nitrogen atoms are not bound to the nearest Zn atoms in the $+2$ charge state, we cannot comment about the split interstitial configuration explicitly. Since the simulation started with a N_2 dimer at a Se site within an otherwise ideal (nondistorted) ZnSe host lattice we assume that the atomic configuration shown in this work is actually the most stable one. We note that in the configuration shown here the N_2 dimer is also oriented along the [100] direction.

VI. CODOPING WITH CL AND IN

The preceding sections showed that compensation and, more severely, degradation phenomena in ZnSe-based devices, are most likely strongly determined by the kinetic formation of stable complexes that form out of the thermodynamically unstable nitrogen acceptor. We can imagine two strategies to avoid, or at least alleviate, these problems: First one could try to reduce the stability of the (N_i-V_{Se}) complex by codoping of donors. The second strategy employs an addition of Te to ZnSe in order to influence the host lattice itself. These two possibilities will be investigated in this and the following sections.

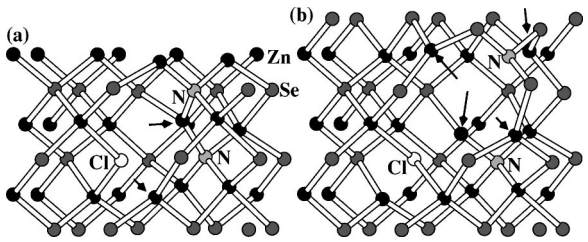

FIG. 14. Ball and stick models for ZnSe codoped with N and Cl: (a) the complex being singly negatively charged; (b) the complex triply positively charged with one nitrogen migrated to an interstitial site.

Recently the enhancement of *p*-type doping in ZnSe by codoping, i.e., doping with *p*- and *n*-type dopants at the same time, was proposed. Katayama-Yoshida and Yamamoto[36] suggested the use of In as the *n*-type dopant from *ab initio* electronic structure calculations. The main focus of their work was to study the influence of codoping on acceptor concentration and mobilities. The aim of our present work is somewhat different. We investigate whether codoping can prevent the decay of the nitrogen acceptor described above. Aside from In, Cl was considered as a possible *n*-type dopant, since it is commonly used for the *n*-type doped layers of ZnSe-based diodes.

A. Codoping with N and Cl

For the case of codoping with Cl, a complex with the two nitrogen atoms connected via a bridging Zn atom and a Cl atom on the Se site closest to the nitrogen was considered. Such a compact complex is expected to be most favorable energetically, since the two negatively charged ionized nitrogen atoms are expected to be attracted by the positively charged ionized Cl atom. The geometry of this complex is shown in the left panel (a) of Fig. 14 for a total charge of -1. The right panel (b) in the same figure features the threefold positive complex with one nitrogen atom at an interstitial site. The respective defect energies are plotted in Fig. 15 as a function of the electronic chemical potential μ_e. In this figure the dashed lines denote the ideal complex with the N and Cl atoms at substitutional sites, and the solid lines the complex with one nitrogen removed to an interstitial site. The energy of the neutral complex with all dopant atoms at substitutional sites has been chosen as the energy zero.

In Fig. 15 the lines denoting the negative charge states for the ideal and decayed cases are almost congruent. This signifies a relaxation of the nitrogen that was initially placed at an interstitial position back to the substitutional site. Therefore, the decayed complex is only stable when carrying a positive charge.

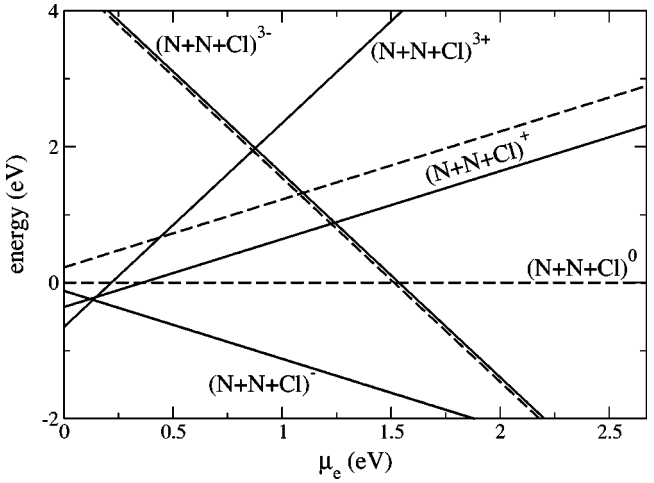

FIG. 15. Defect formation energies for ZnSe codoped with N and Cl. The dashed lines represent the case depicted in the left panel (a) of Fig. 14. The solid lines represent the case of one nitrogen being removed to an interstitial site, such as shown in the right panel (b) of Fig. 14. For a singly negative complex, the dashed and solid lines cannot be separated since they are almost equal in energy.

Apparently even in the ideal case, depicted in panel (a) of Fig. 14, the doping complex distorts the ZnSe lattice considerably. The two Zn atoms that have been marked with arrows in this panel signify this distortion. From the Zn atom connecting the two nitrogen atoms, three bonds protrude which are almost coplanar. The same effect can be seen on one Zn atom to which in the undistorted lattice the Cl atom should have been bound. It appears that the Cl atom is in fact negatively charged, and the two Zn atoms pointed at by arrows compensate for this by carrying the appropriate positive charge.

Figure 15 reveals that the threefold positive complex is energetically favorable with respect to the singly negative one when the electronic chemical potential μ_e approaches the valence-band edge. Therefore, this codoping strategy fails to prevent nitrogen from migrating to an interstitial site even for the threefold positively charged complex, since it may act as a compensating defect. This situation is similar to that encountered with the decay of the nitrogen acceptor that has been described in great detail above. Figure 14 reveals that the stability of interstitial nitrogen with the N+N+Cl complex is caused by the same effect as in the nitrogen-only case, namely, the formation of N-Se bonds together with the subsequent transition of Zn atoms from sp^3 to sp^2 hybridizations. The arrows in the right (b) panel of Fig. 14 indicate these Zn atoms. The decay modes in the present case of codoping and the pure nitrogen acceptor are quite similar, even with respect to the value of μ_e where the -1 and $+3$ charge states cross in Fig. 15. Again a nitrogen atom assumes the role of a donor that compensates for the *p*-type doping. Codoping with Cl could only succeed in prevening the degradation of the dopant if the acceptorlike doping complex turns out to be more stable than the donorlike one. Although we have not considered the fivefold positive decayed N+N+Cl complex, we can conclude that this prerequisite is not met here. Therefore, the presence of Cl atoms as codopants is not sufficient to stabilize the *p*-type doping complex against decay. This result shows that codoping with nitrogen and Cl is not a useful means to suppress the degradation of the *p*-type dopant in ZnSe.

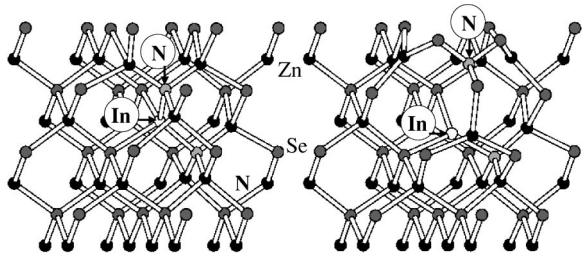

FIG. 16. Ball-and-stick models for the codoping complex formed by two nitrogen atoms and an In atom. Left: ideal configuration with all doping atoms at their respective substitutional sites. Right: one nitrogen atom removed to an interstitial site.

B. Codoping with N and In

The dopant complex formed by two nitrogen atoms and an In atom is identical to that already proposed by Katayama-Yoshida and Yamamoto[36] and consists of two nitrogen atoms at Se sites and one In atom at a Zn site bridging between the two nitrogens. The left panel of Fig. 16 presents a ball and stick model of this complex. As described in the previous sections we investigated the stability of this complex with respect to the migration of one nitrogen atom to a neighboring interstitial site, and the subsequent decay of the acceptor. The results of this investigation are shown in Fig. 17.

In this figure again the formation energies of the doping complex are plotted as functions of the electronic chemical potential μ_e in the host crystal. Dashed lines represent different charge states of the ideal doping complex with every

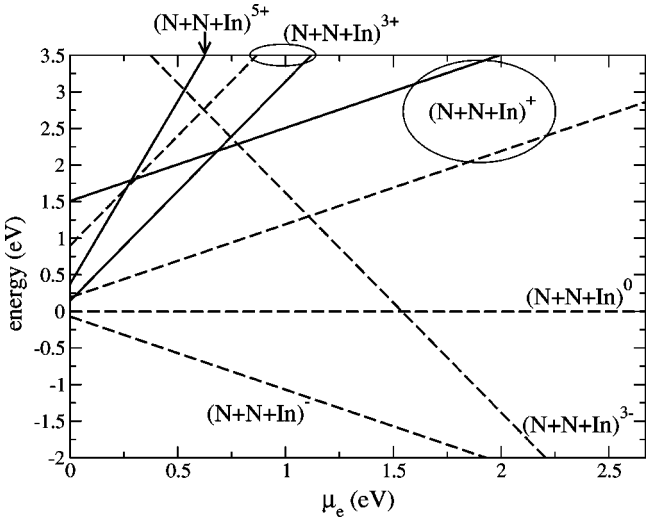

FIG. 17. Formation energies for ZnSe codoped with nitrogen and In. Dashed lines denote an ideal doping complex (left panel in Fig. 16), and solid lines a decayed complex with one nitrogen atom at an interstitial site (right panel in 16).

atom occupying its respective substitutional site (the left panel in Fig. 16). The solid lines denote charge states of the decayed doping complex (the right panel in Fig. 16). The neutral state of the ideal complex has been chosen as the reference state.

In the case of an ideal doping complex (dashed lines) the situation is very similar to an isolated substitutional nitrogen atom. The lines describing the -1, neutral, and $+1$ states intersect near the left edge of the visible range of μ_e, i.e., near the valence-band edge. This shows that the N+N+In codoping complex is an effective *p*-type dopant in its ideal (nondecayed) configuration.

In contrast to the previous case of codoping with Cl, the present doping complex does not decay by nitrogen migration to interstitial sites. This is apparent from the fact that all lines in Fig. 17 describing the decayed doping complex run above those denoting the ideal complex in its neutral and negatively charged states. Therefore, nitrogen migration should not occur since it is energetically unfavorable. Regarding the different charge states of the decayed complex, the $3+$ state is the most stable one since it lies lowest in energy. Since the $1+$ and $5+$ charge states are both higher in energy, we assume that nitrogen migration into an interstitial site is not energetically favorable at any charge state, and is thus suppressed for the N+N+In doping complex. Nevertheless, the present calculations predict the energy difference between the ideal 1- and the decayed $3+$ complexes to be only 0.21 eV in favor of the former. This value is on the same order of magnitude as the uncertainty of the formation energy of the nitrogen-related doping complexes discussed in this work. Therefore, the possibility of a dopant degradation by nitrogen migration cannot be ruled out entirely in the present case.

Unfortunately we cannot decide whether an additional stablilization of the decayed N+N+In complex at a charge of $+5$ by the formation of additional sp^2-hybridized Zn atoms takes place, similar to the case of a single interstitial nitrogen atom (compare Fig. 7). The reason for the is that the supercell chosen for the present investigation is not large enough to simulate atomic displacements in the intermediate neighborhood of the decayed complex. Therefore, the defect formation energies shown in Fig. 17 for the decayed complex at the $5+$ charge state can only be seen as upper limits to the true formation energies.

We point out here that in a real device the stabilization due to the N+N+In doping complex shown here depends on whether this complex actually forms in a sufficiently high concentration during the growth of a *p*-type codoped ZnSe layer. (In the present work it is assumed implicitly that it is already present, without regard to the probability of its formation.) If this were not the case, isolated nitrogen atoms would be embedded in the host lattice, and subsequently subject to the degradation outlined above. From this it follows that the nitrogen and In atoms must be rather mobile during growth in order to form this complex instead of being incorporated into the host lattice independently. It is yet unclear whether this prerequisite is met in customary ZnSe growth.

From these results we conclude that codoping with N and In inhibits the decay of the *p*-type doping in ZnSe by forming a stable acceptorlike complex. Therefore, codoping of ZnSe with In provides a possible means of suppressing the decay of the nitrogen acceptor. The applicability of this means depends yet on the formation of the N+N+In doping complex during growth. It is unclear whether this actually takes place when a ZnSe crystal is grown. Hence we cannot decide here whether the codoping approach to suppress degradation in ZnSe-based devices is a working solution or not.

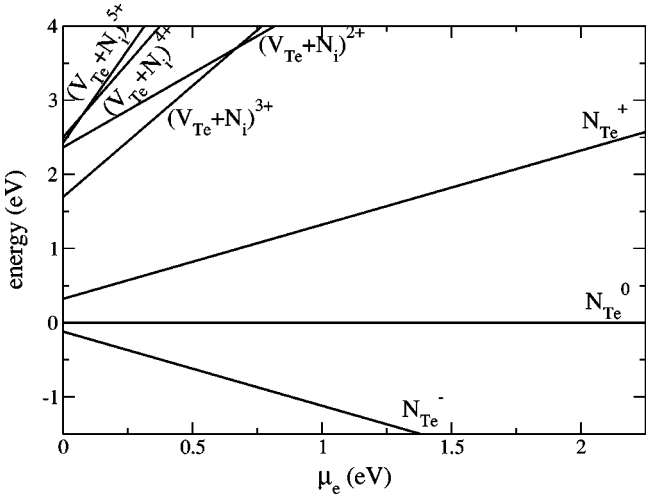

FIG. 18. Formation energies for nitrogen-related point defects in ZnTe. The configurations referred to are similar to those appearing in Fig. 1 and 3.

VII. NITROGEN IN ZNTE: RESULTS FROM THEORY AND EXPERIMENTS

While the achievement of hole concentrations up to 10^{18} cm^{-3} in ZnSe required a considerable effort, it is known that ZnTe can be p-type doped far more easily. In fact, hole concentrations up to 10^{20} cm^{-3} were obtained.[37,38] In addition, Ref. 38 stated that even a small admixture of Te to ZnSe improves the *p*-type dopability with nitrogen significantly in short-period ZnSe/ZnTe superlattices. In the doping experiments described there, a dc plasma source with comparatively low power (15 W) was employed, while nitrogen doping in pure ZnSe is usually done with a high power electron cyclotron resonance or radio frequency plasma source. These observations led us to raise the question of whether the stability of the dopant can also be improved in this way.

Consequently we have calculated formation energies for nitrogen in ZnTe at substitutional Te and interstitial sites similar to those described above for ZnSe. However, only the most significant cases have been considered here. Figure 18 shows the formation energies of all configurations for nitrogen in ZnTe that were investigated in this work. These were corrected similar to ZnSe, also assuming a doping level of 1×10^{17} cm^{-3}. We note here that even applying the Leslie-Gillan correction alone would not shift any of the $(V_{\mathrm{Te}}+N_i)$ instances below the $(N_{\mathrm{Te}})^-$ line. The lines referring to the complex of interstitial nitrogen near a Te vacancy remain above those denoting substitutional nitrogen at a Te site over the full range of the electronic chemical potential. Thus it

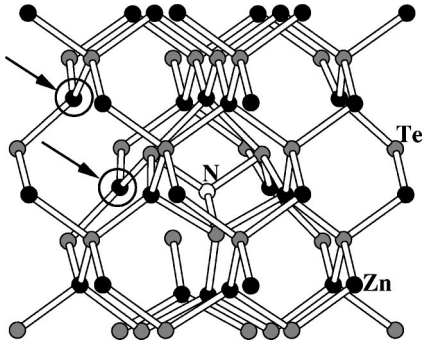

FIG. 19. Ball-and-stick model of a complex featuring an interstitial nitrogen atom and a Te vacancy in ZnTe at the charge state $+5$.

becomes immediately clear that the kind of defect that causes the degradation of nitrogen doping in ZnSe, is not energetically favorable at all in ZnTe.

In the case of substitutional nitrogen the N-Zn bond length varies between 2.021 Å for the -1 and $+1$ charge states and 2.026 Å for the neutral case. After having moved to the interstitial site the nitrogen is bonded to three Te atoms, similar to the situation in ZnSe. The N-Te bond lengths are 2.381, 2.265, 2.243, and 2.235 Å for the $+2$, $+3$, $+4$, and $+5$ cases, respectively.

From these geometrical data the following conclusions can be drawn: When nitrogen is incorporated into ZnTe at a substitutional site the length of the N-Zn bond is equal to that in ZnSe. This implies that the ZnTe lattice is more distorted around the nitrogen site than the ZnSe lattice due to the larger lattice constant of the former. When the nitrogen atom migrates to an interstitial site, the N-Te bond is almost equal in length for the charge states $+3$, $+4$, and $+5$. A shortening of the bond such as appeared in ZnSe is not observed here. This means that the additional stabilization of the interstitial nitrogen in the $+5$ case does not take place in ZnTe. This observation is supported by Fig. 19. The Zn atom indicated to by the lower arrow that borders at the Te vacancy is mainly sp^2 hybridized, since its bonds to the nearest Te atoms are almost coplanar. The Zn atom marked by the upper arrow is mainly sp^3 hybridized, in contrast with the same situation in ZnSe as shown in Fig. 7.

The instability of interstitial nitrogen can be attributed at least in part to the minor strength of the N-Te bond. While no information about the actual strength of this bond are available, the respective values for N-S and N-Se are 4.82 and 3.84 eV in the respective diatomic moelcules.[26] This monotonic decrease suggests that the N-Te bond will be still weaker.

Estimating the effect of the lattice energy to the destabilization of the interstitial nitrogen is difficult. On the one hand the larger lattice constant of ZnTe leads to an increased elastic energy due to the enhanced lattice distortion around the nitrogen site. On the other hand, the ZnTe lattice is less rigid than the ZnSe lattice, thus offering less resistance to distortion. Since the migration of a nitrogen dopant atom from a substitutional to an interstitial site is energetically unfavorable in ZnTe, a possible remedy for the instability of nitrogen as a dopant in ZnSe is the use of ZnTe as a substitute.

While a light-emitting device containing pure ZnTe is difficult to design, the increased stability of a ZnMgCdSe/ZnMgSeTe-based light-emitting diode on an InP substrate was recently demonstrated.[15] In this device the ZnMgSeTe layers were *p* type doped using a rf plasma source. Capacitance-voltage measurements revealed a free hole concentration of up to 10^{18} cm^{-3}. This device was operated at a current density of 50 $Å/cm^2$ for 150 h before it died due to a catastrophic destruction of the gold contact on top of the *p*-type layers.

The superior lifetime of this device can be attributed to two effects: (a) the suppression of nitrogen dopant degradation due to the admixture of about 25% Te in the *p*-type layer, and (b) the use of a tensile strained quantum well that hinders the incoporation of group-VI vacancies diffusing toward it. Since during the operation of the device no change in the microscope picture of the light-emitting area could be observed, we conclude from this experiment that the nitrogen dopant is not susceptible to degradation via the migration to interstitial sites if the Te content in the *p*-type layer is sufficiently high.

VIII. CONCLUSIONS

In the present work a mechanism for the degradation of a nitrogen dopant in ZnSe was presented. It consists of the migration of the dopant atom from the substitutional Se site to a neighboring interstitial site, leaving a vacancy. Such a defect becomes stable only if it is multiply positively charged, thus acting as a donor that compensates for the *p*-type dopant. This degradation mechanism does not assume the diffusion of any other species in the ZnSe lattice, and is thus conceptionally simple. It was shown that the main reason for the stability of the interstitial nitrogen is the formation of N-Se bonds.

Aside from the formation of this interstitial-vacancy complex, the diffusion of its two constituents was investigated. It was found that the diffusion of atomic nitrogen between interstitial sites in ZnSe is hindered by an energy barrier of at least 3.2 eV. On the other hand, the diffusion barrier for the Se vacancy is below 2 eV. Thus it was concluded that, in the experimentally observed diffusion of point defects toward the active region of a ZnSe-based light-emitting device, Se vacancies are the diffusing species.

Aside from atomic nitrogen the behavior of a N_2 molecule incorporated into ZnSe was investigated. A strong dependence on the charge state of the N_2-related defect was observed. N_2 is most stable in the $+2$ state where it also acts as a donor and thus as a compensating defect for *p*-type doping.

Following recent suggestions of the improvement of *p*-type doping by codoping the properties of defect complexes involving Cl or In together with nitrogen were investigated. It was found that codoping with In can inhibit the nitrogen dopant decay by migration to an interstitial site, since the degraded dopant complex is less stable than the intact one. On the other hand, codoping with Cl does not suppress the decay of the nitrogen acceptor.

TABLE III. Corrections to the defect energies in eV for different charge states. The second column gives the correction suggested by Leslie and Gillan while the following columns give the final values of the correction suggested in the present paper for three different charge carrier concentrations. The last row contains the value of the dimensionless parameter γ for the different charge-carrier concentrations [cf. Eq. (A3)].

Defect Charge	Leslie-Gillan Correction	n_0 (cm^{-3}) 1×10^{16}	1×10^{17}	4×10^{17}
1	0.2031	0.1623	0.07396	0.05518
2	0.8124	0.6490	0.2958	0.2207
3	1.828	1.460	0.6656	0.4966
4	3.249	2.596	1.183	0.8829
5	5.077	4.056	1.849	1.380
6	7.311	5.841	2.662	1.987
7	9.952	7.950	3.624	2.704
γ	—	0.0041	0.041	0.163

Finally, it was demonstrated that the decay mode that destabilizes nitrogen in ZnSe does not occur in ZnTe, since interstitial nitrogen is always less stable that that substituting a Te atom. This is accounted for in part by the inferior stability of the N-Te bond, compared to the N-Se bond. The superior lifetime of a light emitting diode whose *p*-type layer consists of ZnMgSeTe can be attributed at least in part to the absence of nitrogen dopant decay.

APPENDIX: FORMATION ENERGY SHIFT DUE TO SCREENING

Within the supercell geometry, employing periodic boundary conditions, it is not possible to simulate charged systems, since the Coulomb repulsion between the cells would diverge, leaving the energy per cell ill defined. The common way to establish charge neutrality is to neglect the $n(\mathbf{G}=\mathbf{0})$ contribution to the Coulomb energy when evaluated in reciprocal space. This is equivalent to introducing a homogeneously distributed background charge (''jellium'') that compensates for the net charge within the supercell.

The remaining interactions between supercells are now short ranged. Especially when the supercell has a simple cubic shape, the remaining interactions can be shown to scale as L^{-5} with the edge L of the cube.[39] Leslie and Gillan[27] suggested using the energy of a simple cubic array of point charges q immersed in a neutralizing background,

$$\Delta E = \frac{q^2\alpha}{2\varepsilon L}, \tag{A1}$$

where ε is the dielectric constant of the host material and α is the Madelung constant, being 2.8373 for a simple cubic supercell of edge length L. This expression was later augmented by Makov and Payne,[28] who included the interaction of the quadrupole moment of the charged defect with a compensating background. It is worth noting here that the main contribution to this correction stems from the interaction between the point charge in one cell and the compensating background in the same cell; in the case of a cubic cell this amounts to about 84% of the value given by Eq. (A1).

While this correction can be used to compute the energy of a single isolated charged point defect in the limit $L\to\infty$, the physical relevance of the situation thus described appears questionable. A semiconductor containing ionized dopant atoms is still neutral as a whole. This raises the question of how the excess charge is distributed within the host crystal. At this point we adopt the formalism describing the screening of an ionized impurity in a non degenerate semiconductor.[40] If the potential of the ionized impurity varies slowly in space, the following approximate differential equation holds:

$$\nabla^2 V \simeq \frac{4\pi n_0 e^2}{\varepsilon k_B T} V = q_D^2 V. \tag{A2}$$

Here n_0 is the density of free carriers within the host material, e the electron charge, ε is again the dielectric constant, $k_B T$ denotes the (thermodynamic) temperature, and q_D is the inverse of the Debye length. This assumption is valid as long as

$$\gamma := \frac{\pi\hbar^2 n_0 e^2}{\varepsilon m^* (k_B T)^2} \ll 1. \tag{A3}$$

Here m^* is the effective electron mass. Equation (A2) can be solved in three dimensions under the assumption of sperical symmetry, yielding a Yukawa potential

$$V(r) = Q/r \exp(-q_D r), \tag{A4}$$

Q being the charge of the impurity. Applying Poisson's equation yields the charge density around the impurity:

$$\rho(r) = \frac{Q q_d^2}{4\pi r} \exp(-q_D r). \tag{A5}$$

Assuming the charged impurity to be point like, its interaction with the surrounding charge density yields

$$E_{\text{int}} = Q^2 q_D. \tag{A6}$$

We proceeded by adding the correction in Eq. (A1) to each formation energy, and afterward subtracting the energy given by Eq. (A6). Here we made the somewhat arbitrary assumptions of room temperature and a density of free carriers of $n_0 = 10^{17}$ cm^{-3}, which describe approximately a typical *p*-type doped ZnSe layer. This corresponds to a Debye length of $q_D^{-1} \simeq 11$ nm. For these values the parameter γ [see Eq. (A3)] is about 0.04, and thus substantially smaller than unity.

In order to clarify the impact of the correction suggested here on the defect energies presented above, we compile the data in Table III. For several defect charges this gives our suggested final correction for three different doping levels. In addition, we plot the three most prominent lines from Fig. 3 for each case occurring in Table III. It can be seen in Fig. 9 that when the correction of Leslie and Gillan is applied, the decayed complex is energetically unfavorable over the whole range of μ_e for both charge states $+3$ and $+5$. Conse-

quently the decay of the nitrogen acceptor as outlined in the present paper should not occur at all. If, on the other hand, we apply the correction of Eq. (A6) in addition to Eq. (A1), and assume a hole concentration of 1×10^{16} cm^{-3}, the decayed complex carrying three positive charges becomes lowest in energy at the left edge of μ_e. At higher assumed hole concentrations the decayed dopant complex becomes increasingly more dominant.

[1] E. Kato, N. Noguchi, M. Nagai, H. Okuyama, S. Kijima, and A. Ishibashi, Electron. Lett. **34**, 282 (1998).

[2] D. Albert, J. Nürnberger, V. Hock, M. Ehinger, W. Faschinger, and G. Landwehr, Appl. Phys. Lett. **74**, 1957 (1999).

[3] M. Adachi, Z.M. Aung, K. Minami, K. Koizumi, M. Watanabe, S. Kawamoto, T. Yamaguchi, H. Kasada, T. Abe, K. Ando, K. Nakano, A. Ishibashi, and S. Itoh, J. Cryst. Growth **214/215**, 1035 (2000).

[4] C.G. Van de Walle, D.B. Laks, G.F. Neumark, and S.T. Pantelides, Phys. Rev. B **47**, 9425 (1993).

[5] S. Pöykkö, M.J. Puska, and R.M. Nieminen, Phys. Rev. B **57**, 12 174 (1998).

[6] D.B. Laks, C.G. Van de Walle, G.F. Neumark, P.E. Blöchl, and S.T. Pantelides, Phys. Rev. B **45**, 10965 (1992).

[7] A. García and J.E. Northrup, Phys. Rev. Lett. **74**, 1131 (1995).

[8] B.-H Cheong, C.H. Park, and K.J. Chang, Phys. Rev. B **51**, 10 610 (1995).

[9] D.J. Chadi and K.J. Chang, Appl. Phys. Lett. **55**, 575 (1989).

[10] M. Kubo, J. Appl. Phys. **78**, 7088 (1995).

[11] H. Kobayashi, K. Kimura, F. Nishiyama, S. Miwa, and T. Yao, J. Cryst. Growth **184/185**, 475 (1998).

[12] E. Tournié, C. Morhain, G. Neu, and J.-P. Faurie, Phys. Rev. B **56**, R1657 (1997).

[13] S. Gundel, D. Albert, J. Nürnberger, and W. Faschinger, Phys. Rev. B **60**, R16 271 (1999).

[14] D. Albert, B. Olszowi, W. Spahn, J. Nürnberger, K. Schüll, M. Korn, V. Hock, M. Ehinger, W. Faschinger, and G. Landwehr, J. Cryst. Growth **184/185**, 571 (1998).

[15] W. Faschinger and J. Nürnberger, Appl. Phys. Lett. **77**, 187 (2000).

[16] P. Hohenberg and W. Kohn, Phys. Rev. **136**, B864 (1964); W. Kohn and L.J. Sham, Phys. Rev. **140**, A1133 (1965).

[17] J.P. Perdew and A. Zunger, Phys. Rev. B **23**, 5048 (1981); D.M. Ceperley and B.J. Alder, Phys. Rev. Lett. **45**, 566 (1980).

[18] R.P. Feynman, Phys. Rev. **56**, 340 (1939).

[19] M. Bockstedte, A. Kley, J. Neugebauer, and M. Scheffler, Comput. Phys. Commun. **107**, 187 (1997); also see http://www.fhi-berlin.mpg.de/th/th.html

[20] D.R. Hamann, Phys. Rev. B **40**, 2980 (1989).

[21] N. Troullier and J.L. Martins, Phys. Rev. B **43**, 1993 (1991).

[22] S.G. Louie, S. Froyen, and M.L. Cohen, Phys. Rev. B **26**, 1738 (1982).

[23] X. Gonze, P. Käckell, and M. Scheffler, Phys. Rev. B **41**, 12 264 (1990).

[24] M. Fuchs and M. Scheffler, Comput. Phys. Commun. **119**, 67 (1999).

[25] *Semiconductors Physics of II-IV and I-VII Compounds, Semimagnetic Semiconductors*, edited by O. Madelung, Landolt Börnstein New Series, Group III, Vol. 17, Pt. 1 (Springer-Verlag, Berlin 1982).

[26] *CRC Handbook of Chemistry and Physics*, 75th ed. eidted by D. R. Lide (CRC, Boca Raton, FL, 1994).

[27] M. Leslie and M.J. Gillan, J. Phys. C **18**, 973 (1985).

[28] G. Makov and M.C. Payne, Phys. Rev. B **51**, 4014 (1995).

[29] I.S. Hauksson, J. Simpson, S.Y. Wang, K.A. Prior, and B.C. Cavenett, Appl. Phys. Lett. **61**, 2208 (1992).

[30] K.W. Kwak, R.D. King-Smith, and D. Vanderbilt, Phys. Rev. B **48**, 17 827 (1993).

[31] B. v. Tschirschnitz-Geibler, *Gmelin Handbook of Inorganic Chemistry, Subvolume B1 Selenium*, 8th ed.

[32] R. W. G. Wyckoff, *Crystal structures*, 2nd ed. (John Wiley & Sons, New York, 1963).

[33] L.C. Kimerling, Solid-State Electron. **21**, 1391 (1978).

[34] A.L. Chen, W. Walukiewicz, K. Duxstad, and E.E. Haller, Appl. Phys. Lett. **68**, 1522 (1996).

[35] E. Kurtz, D. Albert, J. Kraus, D. Hommel, and G. Landwehr, in *Proceedings of the International Symposium on the Blue Laser and Light emitting Diodes* (Chiba University, Japan, 1996), p. 429.

[36] H. Katayama-Yoshida and T. Yamamoto, Phys. Status Solidi B **202**, 763 (1997).

[37] I.W. Tao, M. Jurkovic, and W.I. Wang, Appl. Phys. Lett. **64**, 1848 (1994).

[38] W. Faschinger, S. Ferreira, and H. Sitter, Appl. Phys. Lett. **64**, 2682 (1994).

[39] N. W. Ashcroft and N. D. Mermin, *Solid State Physics* (Saunders, Philadelphia 1976).

[40] W. Jones and N. H. March, *Theoretical Solid State Physics*, 2nd ed. (Dover, New York 1985), Vol. 2.